HHS Public Access

Author manuscript

Microbes Infect. Author manuscript; available in PMC 2017 November 01.

Published in final edited form as:

Microbes Infect. 2016 November ; 18(11): 675–686. doi:10.1016/j.micinf.2016.06.006.

Antagonistic Effect of Atorvastatin on High Fat Diet Induced Survival during Acute Chagas Disease

Dazhi Zhao[a], **Kezia Lizardo**[b], **Min Hui Cui**[c,d], **Kamalakar Ambadipudi**[c,d], **Jose Lora**[a], **Linda A Jelicks**[d,e], and **Jyothi F Nagajyothi**[a,b,*]

[a]Department of Pathology, Albert Einstein College of Medicine, 1300 Morris Park Avenue, Bronx, NY -10461

[b] Department of Microbiology, Biochemistry and Molecular Genetics, Public Health Research Institute, Rutgers state University, 225 Warren Street, Newark, NJ -07103

[c]Department of Radiology, Albert Einstein College of Medicine, 1300 Morris Park Avenue, Bronx, NY -10461

[d]Department of Physiology and Biophyiscs, Albert Einstein College of Medicine, 1300 Morris Park Avenue, Bronx, NY -10461

[e]Department of The Gruss Magnetic Resonance Research Center, Albert Einstein College of Medicine, 1300 Morris Park Avenue, Bronx, NY -10461

Abstract

Chagasic cardiomyopathy, which is seen in Chagas Disease, is the most severe and life-threatening manifestation of infection by the kinetoplastid *Trypanosoma cruzi*. Adipose tissue and diet play a major role in maintaining lipid homeostasis and regulating cardiac pathogenesis during the development of Chagas cardiomyopathy. We have previously reported that *T. cruzi* has a high affinity for lipoproteins and that the invasion rate of this parasite increases in the presence of cholesterol, suggesting that drugs that inhibit cholesterol synthesis, such as statins, could affect infection and the development of Chagasic cardiomyopathy. The dual epidemic of diabetes and obesity in Latin America, the endemic regions for Chagas Disease, has led to many patients in the endemic region of infection having hyperlipidemia that is being treated with statins such as atorvastatin. The current study was performed to examine using mice fed on either regular or high

[*]**Corresponding Address**: Jyothi F Nagajyothi, 225, Warren Street, Newark, NJ- 07103, Telephone: 973-854-3450, Fax: 973-854-3101, jfn31@njms.rutgers.edu.

Gene List with NCBI accession number.

Cxcl16 NM_023158.6, Stab1 NM_138672, Vldlr NM_013703, Lrp6 NM_008514, Ldlr NM_010700, Scarf1NM_001004157, Apoa1NM_009692, Apob NM_009693, Apoe NM_009696, Acaa1aNM_130864, Acad9 NM_172678, Acad10NM_028037, Acox1NM_015729, Fabp1NM_017399, Acsbg1NM_053178, Lipe NM_010719, Npc1NM_008720, Lcat NM_008490, Abca1 NM_013454, Abcg1NM_009593, Cyp39a1NM_018887, Cyp7a1NM_007824, Hmgcr NM_008255, Insig1NM_153526, Lep NM_008493, Ppara NM_011144, Pparg NM_011146, Adig NM_145635, Adipoq NM_009605

6. **CONFLICT OF INTEREST STATEMENT**

None of the authors have conflict of interest.

fat diet the effect of atorvastatin on *T. cruzi* infection-induced myocarditis and to evaluate the effect of this treatment during infection on adipose tissue physiology and cardiac pathology. Atorvastatin was found to regulate lipolysis and cardiac lipidopathy during acute *T. cruzi* infection in mice and to enhance tissue parasite load, cardiac LDL levels, inflammation, and mortality in during acute infection. Overall, these data suggest that statins, such as atorvastatin, have deleterious effects during acute Chagas disease.

Keywords

Chagas disease; cardiomyopathy; high fat diet; adipose tissue; lipidopathy; metabolic disorder

1. INTRODUCTION

Chagas disease is caused by a parasite *Trypanosoma cruzi*, and it is estimated that more than 100 million people are currently at risk of becoming infected [1]. Chagas disease is a major cause of mortality and morbidity in Latin America, largely due to cardiomyopathy that develops in a large segment of the infected population [1, 2]. Recent research has demonstrated that *T. cruzi* causes a significant infection in adipocytes and adipose tissue, resulting in changes in adipocyte physiology that affects parasitemia, tissue parasite loads and cardiac pathology [2-4]. A western-style diet that is high in fat and processed foods is becoming prevalent in Latin America, replacing the traditional dietary system, and has been accompanied by an increased incidence of diabetes and obesity in this Chagas Disease endemic region. This increase in obesity may have significant effects on the pathogenesis of Chagas Disease and have spurred investigation into the interaction between diet, host adipocyte physiology, lipid homeostasis, and Chagas disease. However, many aspects of this interaction still remain unknown.

Chagas disease has three described phases during infection – the acute phase, characterized by myocarditis, fever and hepatomegaly, the indeterminate phase that is characterized by a lack of disease symptoms, and the chronic phase, which develops in approximately 30% of infected individuals and is characterized by the development of cardiomyopathy. Previous studies have demonstrated that in a murine model of acute Chagas disease, high fat diet (HFD) has a protective effect during infection, resulting in increased survival [2, 5]. In addition, in mice fed a regular diet (RD), *T. cruzi* infection causes significant lipolysis (60%), which may contribute to cardiac lipidopathy and high parasite loads during acute infection [2]. In contrast, HFD ameliorates the effects of infection of adipose tissue and reduces adipocyte lipolysis [2]. Infected mice fed on an HFD also have improved cardiac pathology compared to infected mice fed on a RD. It has also been demonstrated that *T. cruzi* has a high affinity for lipoproteins and that the invasion rate of this parasite increases in the presence of cholesterol [6-8], suggesting that drugs that inhibit cholesterol synthesis, such as statins, may affect infection progression. It has been demonstrated that statins have a potential beneficial effect on the progression of cardiomyopathy in dogs at chronic stages of Chagas disease [10]; however, whether statins affect other stages of Chagas disease has not been explored. This line of inquiry is motivated by the fact that approximately 24.1 million people with diabetes and various associated lipid disorders live in Latin America, the

endemic region for Chagas Disease, and that many of these patients take statins for hyperlipidemia [9].

In this study we analyzed the effect of HFD in combination of atorvastatin (marketed as Lipitor in the United States) on adipocyte physiology and function, and its relation to cardiac pathology using a murine acute Chagas model that was fed either a HFD or RD. The effect of atorvastatin on adipose tissue was analyzed at the early acute infection stage (d10pi) as we have previously determined that adipose tissue significantly responds to infection at this time point [4]. Treatment with atorvastatin was found to increase lipolysis and caused enhanced lipid accumulation, inflammation and parasite load in the hearts of infected animals. The known effect of atorvastatin to increase LDL receptors in both adipose tissue and heart is likely results in a higher parasite load when this drug is used in acute *T. cruzi* infection. In addition, atorvastatin treatment results in an elevated mortality rate during acute infection in the murine CD1 Chagas model. Together, these results indicate that statin drugs may adversely impact the progression of acute Chagas disease.

2. MATERIALS AND METHODS

2.1 Ethical approval

All animal experimental protocols were approved by the Institutional Animal Care and Use Committee (IACUC) of the Albert Einstein College of Medicine (No. 20130202) and adhere to the National Research Council guidelines (Guide for the Care and Use of Laboratory Animals: Eighth Edition, Washington, DC: The National Academies Press, 2011).

2.2 Experimental animal model

The Brazil strain of *T. cruzi* was maintained by passage in C3H/Hej mice (Jackson Laboratories, Bar Harbor, ME). Male CD-1 mice (Jackson Laboratories) were infected intraperitoneally (i.p.) at 8–10 weeks of age with 5×10^4 trypomastigotes of the Brazil strain [3]. Mice were maintained on a 12-hour light/dark cycle. Mice, starting at the day of infection, were randomly divided into four groups (n = 15 per group) and fed on either high fat diet (HFD; 60% fat D12492 Research Diets, Inc., New Brunswick, NJ) or regular diet (RD, 10% fat D12450 Research Diets, Inc., New Brunswick, NJ) or HFD containing atorvastatin (HFDA 100mg atorvastatin/kg diet) or RD with atorvastatin (RDA 100mg atorvastatin/kg diet) (Research Diets, Inc., New Brunswick, NJ). Uninfected mice were fed on either HFD (n=15) or RD (n=15) or HFDA or RDA and used as respective controls in all the experiments. The experiment was replicated using n=30 mice in all groups.

Plasma samples were obtained from 75 μl of blood collected from the orbital venous sinus (using isoflurane anesthesia) at 10, 15, 20, 25 and 30 days post infection (dpi). Parasitemia was evaluated by counting in a Neubauer hemocytometer as described previously [3]. At days 10, 20 and 35 days after infection the mice were euthanized and heart and epididymal white adipose tissues (WAT) were harvested for analysis. There was no peripheral parasitemia observed at d 35 after infection and mice appeared normal.

2.3 Immunoblot analysis

Tissue lysates were prepared as previously described [2-5]. An aliquot of each sample (40 μg proteins) was subjected to electrophoresis on a 4-15% gradient SDS-PAGE and the proteins transferred to nitrocellulose filters for immunoblot analysis. LDLr specific rabbit monoclonal antibody (1:1000 dilution, AB52818 Abcam, Cambridge, MA), lipoprotein lipase (LPL) specific mouse monoclonal antibody (1:1000 dilution, AB21356, Abcam), adipose triglyceride lipase (ATGL) specific rabbit monoclonal antibody (1:1000 dilution, AB 109251), hormone sensitive lipase (HSL) specific rabbit monoclonal antibody (1:1000 dilution, AB 45422), lipoprotein lipase (LPL) specific mouse monoclonal antibody (1:1000 dilution, AB 21356) or TNF-α specific rabbit polyclonal antibody (1:1000 dilution, AB6671, Abcam) were used as primary antisera. Horseradish peroxidase-conjugated goat anti-mouse immunoglobulin (1:2000 dilution, Amersham Biosciences, Piscataway, NJ) or horseradish peroxidase-conjugated goat anti-rabbit immunoglobulin (1:5000 dilution, Amersham Biosciences) were used to detect specific protein bands (explained in Figure Legends) using a chemiluminescence system [4]. GDI (1: 10000 dilution, 71-0300, and rabbit polyclonal, Invitrogen, CA) and a secondary antibody horseradish peroxidase conjugated goat anti-rabbit (1:2000 dilution, Amersham Biosciences) was used to normalize protein loading.

2.4 Quantitative Determination of Parasite Load in Tissue

Heart and white adipose tissue were collected from mice on 30 days post-infection (pi) and stored at −80 °C. A quantitative real-time polymerase chain reaction (qPCR) was used to quantify parasite load employing PCR SYBR Green Master Mix (Roche Applied Science, CT) containing $MgCl_2$ employing an iQ5 LightCycler (Bio-Rad). Isolation of DNA, preparation of standard curves for host and epimastigote DNA, and qPCR analysis was performed as previously published [14]. Host 18srRNA gene was used for normalization [18S forward: 5′-AGGGTTCGATTCCCGGAGAGG-3′, reverse, 5′-CAACTTTAATATACGCTATTGG-3′].

2.5 Polymerase Chain Reaction Array

An RT^2 Profiler (SA Biosciences, Valencia, CA) custom designed PCR array for mouse genes involved in LDL internalization, cholesterol metabolism, fatty acid and triglyceride metabolism and inflammatory signaling was used to analyze gene expression. Data analysis was performed normalized to the expression of 18sRNA using the ΔΔCT method according to the manufacturer's protocol (SABiosciences) and as previously mentioned [2, 4].

2.6 Immunohistochemistry and Immunofluorescence analysis (IFA)

Freshly isolated tissues were fixed with phosphate-buffered formalin overnight and then embedded in paraffin using standard protocols. Hematoxylin and eosin (H&E) staining was performed and the images were captured as previously published [2]. Four to six sections of each heart were scored blindly. For each myocardial sample, histologic evidence of myocarditis and inflammation was graded on a six point scale ranging from 0 to 5+ as previously published. A zero score indicated lowest or negligible changes and 4 the most damaged state. IFA was performed on the frozen sections using anti-LDL and the images

were captured as previously published [2]. The fluorescent intensities of the images were quantified using NIH-Image J program for four to six images of each heart.

2.7 Magnetic resonance imaging (MRI) analysis

Cardiac gated MRI was performed on uninfected and infected mice at 26 dpi were imaged using a 9.4 T Varian Direct Drive animal magnetic resonance imaging and spectroscopic system (Agilent Technologies, Inc. Santa Clara, CA) as previously published [2, 11]. Briefly, anesthesia was induced with 2% isoflurane in air, mice were positioned supine inside an MR compatible holder and positioned within a 35-mm ID quadrature ^{1}H volume coil (Molecules2Man Imaging Co., Cleveland, OH). Body temperature was maintained at 34 ~35 °C using warm air with feedback from a body surface thermocouple. A respiratory sensor balloon was taped onto the abdomen. Cardiac (ECG electrodes inserted subcutaneously in front left paw and rear right paw) and respiratory signal (from sensor balloon taped to the abdomen) were continuously monitored and used for MR gating/ triggering by an SA Monitoring and Gating System (Small Animal Instruments, Inc., Stony Brook, NY). Ten to fourteen 1-mm-thick slices without gap was acquired in short-axis orientation covering the entire heart using an ECG-triggered and respiratory gated multi-frame tagged cine sequence. The imaging parameters used were field of view (FOV) of 40 × 40 mm^2, matrix size of 256 × 256, TE of 2.6 ms, TR of 5.5 ms, flip angle of 25°, number of averages of 2. The number of frames was twelve to eighteen. Data were transferred to a PC and analyzed using MATLAB-based software. Left ventricle (LV) and right ventricle (RV) dimensions in millimeters were determined from the images representing end-diastole. The left ventricular wall is the average of the anterior, posterior, lateral, and septal walls. The right ventricular internal dimension is the widest point of the right ventricular cavity.

2.8 Statistical Analysis

Immunoblot, immunofluorescence and quantification of parasite load studies were performed at least three times and representative data are presented in the figures. Data were pooled and statistical analysis was performed using a Student's t-test (Microsoft Excel) as appropriate and significance differences were determined as p values between < 0.05 and <0.005 as appropriate. Gene array analyses were done in duplicates as described earlier [4].

3. RESULTS

3.1 Atorvastatin treatment reduces *T. cruzi* parasitemia during acute infection

We evaluated the effect of the cholesterol lowering statin drug atorvastatin (e.g. Lipitor), on parasitemia during acute infection in *T. cruzi* infected mice fed on either RD or HFD. Atorvastatin treated mice displayed a significantly decreased parasitemia when fed either an RD or HFD diet (i.e. RDA and HFDA mice) compared to their respective atorvastatin untreated cohorts (Figure 1A). The highest parasitemia was observed in untreated RD fed infected mice, while the lowest parasitemia was observed in the HFD fed treated (i.e. HFDA) infected mice (Figure 1A, d 15-30).

3.2 Atorvastatin reduces survival during acute *T. cruzi* infection

We found that the anti-cholesterol drug atorvastatin significantly decreased the survival rate in both the RDA and HFDA fed mice compared with untreated mice during acute infection. Infected untreated mice fed on RD and HFD showed 45% and 90% survival rate, respectively, compared with uninfected mice. However, infected atorvastatin-treated mice had even further reduced survival rates: RDA fed mice had a 14% survival rate and HFDA fed mice had a 68% survival rate (Figure 1B). Interestingly, although the parasite load was higher in both the heart and WAT of infected HFDA fed mice compared to the infected RDA fed mice, infected HFDA fed mice still displayed a better survival rate compared to the infected RDA fed mice (presumably due to effects of HFD diet on adipocyte biology and infection as we have previously observed [2]).

3.3 Atorvastatin treatment increases tissue parasitism

We measured tissue parasite loads and quantified them by qPCR analysis [3] in atorvastatin-treated mice and controls. Even though atorvastatin treatment significantly reduced parasitemia during acute infection in both RDA and HFDA fed mice (Figure 1C), it significantly increased parasite loads both in the hearts and WAT compared to atorvastatin untreated infected mice (RD and HFD) at d30pi (this is the point at which we have seen maximal parasite loads in these tissues during acute infection in our previous studies [2, 3]). HFDA mice had the highest levels of parasite loads both in heart and WAT samples compared to all other infected experimental groups. The cardiac parasite levels in HFDA and RDA mice were 251 and 15.7 fold greater compared to respective untreated (HFD and RD fed) infected animals. In the WAT samples of HFDA and RDA infected mice, the parasite loads were 5.5 and 2.7 folds higher compared to their respective untreated HFD and RD fed infected animals (Figure 1C).

3.4 Atorvastatin treatment improves cardiac morphology during acute infection

MRI examination of the heart during both diastole and systole revealed significant alterations in the cardiac morphology in infected mice treated with atorvastatin (Table 1). As we have reported previously acute infection significantly decreased left ventricle internal diameter (LVID) and significantly increased (diastole and systole) the right ventricle internal diameter (RVID) both in RD and HFD fed mice compared to uninfected mice [2]. Atorvastatin treatment significantly alleviated these changes in both LVID and RVID, especially in LVID in RDA fed mice during acute infection. We also found that during acute infection, RD fed mice displayed significantly greater wall thickness (141%) compared to uninfected RD fed mice (100%), while HFD fed mice displayed no significant difference in the wall thickness between infected and uninfected mice. Interestingly, atorvastatin treatment significantly decreased wall thickness in both the RDA (42%) and HFDA (57%) fed mice during acute infection compared to RD and HFD fed uninfected mice (100%) respectively. We also measure fractional shortening (FS%), which was significantly increased in the infected mice. Atorvastatin treated mice showed a significant decrease in FS %, especially in RDA fed mice during infection. Overall, atorvastatin treatment had a beneficial effect on cardiac morphology (Table 1).

3.5 Atorvastatin promotes damage and inflammation of the heart during acute infection (d30pi)

Atorvastatin treatment aggravated inflammation and cardiac damage in both RDA and HFDA mice during acute infection. Comparing the H&E histology of RDA and HFDA infected mouse hearts at d30pi, we found that the hearts of RDA fed mice had significantly greater inflammation and damage compared to the hearts of HFDA fed mice (Figure 2A & 2D). Additionally, DAPI staining of these hearts demonstrated a larger number of amastigote nests in atorvastatin treated infected mice compared to atorvastatin untreated infected mice (Figures 2B & 2D). Comparison of these amastigote nests showed that there were more nests and they were larger in size in the hearts of HFDA fed infected mice compared to RDA fed infected mice (Fig. 2B & 2D, about a 40% increase in infected HFDA compared to RDA mouse hearts). H&E stained cardiac tissues demonstrated an average of 50 to 200μm bigger amastigote nests in HFDA and an average of 30 to 100μm size in RDA fed mice (Supplemental Fig 1&2).

3.6 Atorvastatin treatment increases cardiac LDL levels during infection

Immunofluorescence analysis demonstrated significantly increased cardiac LDL levels in RDA and HFDA fed infected mice compared with atorvastatin untreated RD and HFD fed infected mice (Fig. 2C & 2D). LDL accumulation was higher in HFDA fed mice compared to RDA fed mice (Fig. 2C & 2D).

3.7 Atorvastatin treatment increases tissue LDL receptor levels but reduces scavenger receptor levels during acute infection

It has been shown that atorvastatin treatment increases cell surface LDL receptor levels in various tissues and cells including mononuclear cells [12]. Atorvastatin treatment altered various genes involved in energy metabolism and immunity in mice fed on either a RD or an HFD (Supplemental data: Table. 1). However, mice fed on HFD and treated with atorvastatin (HFDA) showed highly pronounced changes in the expression of these genes both in the WAT and hearts (Supplemental data: Table. 1). Previously we reported that adipose tissue significantly responds to early infection [4]. We therefore evaluated the effect of atorvastatin on LDL receptor levels during infection in WAT at early acute infection (d10 pi) (Fig. 3) [4]. We have previously observed increased parasite load in the heart between d15 and d30pi during acute infection. Therefore, we measured LDL receptor levels in the heart at active acute infection (d20 pi) by immunoblot analysis (Fig.4) [3]. An increased level of LDL receptors (approximately a 1.7- 2.8 fold increase compared to RD fed uninfected mice) was seen in infected WAT in all four infected experimental groups (HFD, HFDA, RD, and RDA). Atorvastatin treatment by itself, in the absence of infection, had no significant effect on the levels of LDL receptors in WAT of RDA fed mice compared to RD fed mice at d10 pi. However, atorvastatin treatment synergistically increased the levels of LDL receptors in WAT of HFDA fed mice compared to HFD fed mice during infection (about a 2 fold increase). Similarly in the heart tissues, infection increased the levels of LDL receptors in all the infected experimental groups. Atorvastatin treated infected mice (RDA and HFDA) had higher levels of LDL receptors (8 and 15 fold respectively,) compared to untreated infected

mice (RD and HFD). Interestingly among the uninfected groups, the HFDA fed mice had higher levels of LDL receptors compared to HFD fed uninfected mice (Figure 3).

qPCR analysis was performed to measure the mRNA levels of LDL receptors and other scavenger receptors such as (Chemokine (C-X-C motif) ligand 16 (CXCL16), VLDLr (Very Low Density Lipoprotein receptor), LRP6 and Stabilin1 (Stab1)) involved in the transportation of LDL and modified LDLs. qPCR analysis performed at the end of acute infection (d30pi, when no significant parasitemia or mortality is observed) confirmed the immunoblot studies and also demonstrated significant foldchange in the mRNA levels of LDL receptors in both WAT and heart tissues at d30 pi (Table 2). WAT samples of HFDA fed infected mice demonstrated significantly upregulated mRNA levels of LDL receptors compared to HFD fed infected mice (Table 2). The mRNA levels of scavenger receptors were significantly altered in both WAT and hearts during infection. HFDA fed mice showed significantly increased mRNA levels of scavenger receptors in WAT samples compared to HFD fed mice at d 30pi (Table 2). WAT samples from RDA fed infected mice had decreased mRNA levels of CXCL16, significantly increased mRNA levels of Stab1 and VLDLr, and no significant difference in the mRNA levels of LRP6 and LDLr compared to RD fed infected mice (Table 2).

In the heart tissues the mRNA expression levels of CXCL16 were significantly higher in both RDA and HFDA fed infected mice compared to their respective atorvastatin untreated infected mice at d30pi (Table. 2). Interestingly, cardiac mRNA levels of other scavenger receptors in the atorvastatin treated infected mice measured were either decreased (in RDA fed infected) or showed no change compared to their levels in the respective untreated infected mice. The only exception to this pattern was in the increased levels (3.2 fold) of VLDLr in the HFDA fed infected group compared to HFD fed infected mice.

3.8 Atorvastatin treatment differentially regulates cholesterol efflux in RDA and HFDA fed mice during acute infection

The qPCR analysis demonstrated differential mRNA expression levels of apolipoproteins and ATP binding cassette A1 and G1 (Abca1 and AbcG1) mRNAs in RDA and HFDA fed mice compared with the respective untreated mice during late acute infection (d30 pi) (Table 2). In the WAT samples from HFDA fed mice Apolipoproteins a1 and b, and Abca1 and Abcg1 were significantly higher compared to RDA fed mice. The mRNA level of Abca1 was significantly lowered in the WAT of RDA fed mice compared to atorvastatin untreated RD fed infected mice as well as to the HFDA fed infected mice at d30 pi (Table 2). However, in cardiac tissue, even though the mRNA levels of Apo a1 and b1 were significantly higher in HFDA fed mice compared to RDA fed mice, the mRNA levels of Abca1 was significantly reduced in HFDA fed mice. These data suggest that the atorvastatin treatment regulates cholesterol efflux mechanism differentially between RDA and HFDA fed mice as well as between different tissues (WAT and heart) during acute *T. cruzi* infection.

3.9 Atorvastatin treatment positively regulates adipogenesis in HFD fed mice during acute infection

We found that atorvastatin treatment further decreased the mRNA expression levels of these adipogenic markers (adiponectin, adipogenin, PPARγ and leptin) in WAT from RDA fed infected mice. However, in the WAT from HFDA fed mice atorvastatin induced a significant increase in the mRNA levels of these adipogenic genes compared to untreated infected mice (Table 2). In contrast to WAT, in cardiac tissue atorvastatin treatment increased adiponectin mRNA levels in mice fed on RD but significantly decreased adiponectin levels in HFD fed mice (Table 2).

3.10 Atorvastatin treatment upregulates cholesterol and fatty acid metabolism in HFD fed mice

We performed qPCR analysis of the genes involved in the cholesterol and fatty acid metabolism to examine the effect of atorvastatin during acute infection on lipid metabolism in infected mice fed on different diets. The mRNA analysis of WAT demonstrated significantly upregulated cholesterol and fatty acid metabolism in HFDA fed infected mice compared to HFD fed infected mice (Table 2). The WAT of RDA fed infected mice showed either no significant difference or decreased levels of mRNAs of the genes involved in fat metabolism compared to untreated RD fed infected mice. We also measured the WAT expression of Cyp7a1 cholesterol 7-alpha-hydroxylase, which is a rate limiting enzyme in the synthesis of bile acid from cholesterol. Atorvastatin treatment increased mRNA levels of Cyp7a1 in both RD and HFD fed mice compared to the corresponding untreated infected mice (Table 2).

3.12 Atorvastatin treatment differentially regulates inflammatory signaling between WAT and hearts in the mice fed on different diets during acute infection

mRNA analysis demonstrated that atorvastatin treatment significantly upregulated mRNA levels of various inflammatory markers in the context of HFD; e.g. interferon gamma (IFNγ), chemokine (C-C motif) ligand 2 and 5 and receptors 1 and 2 (Ccl2 and Ccl5, Cdr1 and Ccr2) and interleukin 1 (Il-1), Ifnγ, Il1a, Tgfb1 and TNFα, in the WAT of infected mice (Table 2). Similarly, atorvastatin treatment caused a significant increase in Ccl5, Ccr2 and Ifnγ in the WAT of RD fed infected mice. The mRNA levels of inflammatory markers were also upregulated by atorvastatin in the hearts of RD fed infected mice. Interestingly, however, the mRNA levels of inflammatory markers were significantly down-regulated by atorvastatin in the hearts of HFD fed infected mice at d30 post infection (Table 2).

3.13 Atorvastatin treatment significantly increases the protein levels of TNFα in WAT during early acute infection

Immunoblot analysis demonstrated a significant increase in the protein levels of TNFα in the WAT of atorvastatin treated infected mice (1.4 fold increase in RDA and 2.3 fold increase in HFDA) compared to the corresponding untreated cohorts (RD and HFD) at the early acute phase of infection (d 10 pi, Figure 4). In particular, HFDA fed mice had a significantly higher expression of TNF relative to all of the other experimental groups during

infection (Figure 4). qPCR analysis also demonstrated increased TNFα levels in HFDA fed mice at d30 pi (Table 2).

3.14 Atorvastatin treatment differentially regulates the levels of various lipases in RD and HFD fed mice during early acute infection

Immunoblot analysis demonstrated that atorvastatin treatment differentially alters the protein levels of lipases (hormone sensitive lipase (HSL), adipose triglyceride lipase (ATGL) and lipoprotein lipase (LPL)) in WAT of infected mice fed on either RD or HFD at d10 pi (early stage of acute infection). Atorvastatin treatment significantly increased ATGL levels and decreased HSL levels in WAT of uninfected mice compared to untreated mice regardless of the type of diet. Atorvastatin treatment significantly increased ATGL in RDA fed infected mice compared to RD fed infected mice. However, no significant change was observed between HFDA and HFD fed infected groups. HSL was significantly increased in HFDA fed infected mice (190 fold increase) compared to HFD fed infected mice and RDA fed infected mice (20 fold increase) compared to RD fed infected mice. Atorvastatin treatment also significantly altered LPL levels in both RDA and HFDA fed infected mice compared to RD and HFD fed infected mice (five-fold decrease in RDA infected mice compared to RD infected mice and 3 fold increase in HFDA infected mice compared to HFD infected mice).

4. DISCUSSION

In this study we investigated the effect of cholesterol-lowering drug atorvastatin (A) taken in combination with regular (RD) or high fat diet (HFD) on several aspects of acute *T. cruzi* infection in the mouse model. Acute *T. cruzi* infection results in 40 to 60% mortality in CD1 mice. We previously demonstrated that HFD increases the survival rate and decreases the cardiac parasite load during acute infection compared to RD mice [2]. We also reported that the treatment with an anti-diabetes drug metformin decreases mortality both in RD and HFD fed *T. cruzi* infected mice compared with metformin untreated infected mice during acute infection [5]. In contrast, we found that atorvastatin increases mortality in *T. cruzi* infected mice during acute infection and treatment with atorvastatin also caused a significant increase in cardiac parasite load and inflammation. While tissue parasite load was increased by atorvastatin treatment, there was a decrease in blood parasitemia and this effect was independent of the type of diet (RD or HFD) the mice were fed (Figure 1). Effect of diet and atorvastatin on lipid metabolism of WAT and heart during acute infection was studied at three different time points. Early acute phase (d 10pi) was chosen to analyze WAT as we have previously demonstrated a significant loss in adipocytes by d 15pi which contributes to the pathogenesis of cardiomyopathy [3, 4, 7].

T. cruzi has high affinity for cholesterol (LDL and HDL) and uses LDL receptors and scavenger receptors to invade various host cells [7, 8, 16, 17]. We measured LDL receptor levels in WAT (d 10pi) and heart (d 20pi) at early acute phase and active acute phase respectively since at these respective time points we observed significant initiation of pathological changes in these tissues (these time points were also chosen to avoid loss of animals due to death from infection) [4, 8]. LDL receptor levels were significantly higher in these tissues and we believe this result in increased invasion by this parasite and leads to the

higher tissue parasite loads in mice given atorvastatin (Fig. 3 & 4). Indeed, we found that adipocytes, which are considered both a target cell and reservoir for *T. cruzi*, demonstrated significantly increased LDL receptor levels, especially at the early stage of infection (at d10 pi) in atorvastatin treated infected mice compared to untreated infected mice (Figure 4). By the end of the acute infection (d30 pi) period when mortality is occuring, the WAT mRNA levels of LDL receptor were significantly decreased in RDA fed infected mice compared to RD fed infected mice. This suggests that atorvastatin treatment probably facilitates parasite invasion into adipose tissue at the early stages of infection. Interestingly, HFDA fed infected mice showed significantly increased mRNA levels of LDL receptor and other scavenger receptors even at d30 pi compared to RDA infected mice. This alteration in the receptor levels in the WAT of HFDA mice may explain the observed persistence of an increased parasite load by the end of acute infection (d 30 pi) in HFDA fed mice (Figure 1). A previous study using a dog model has shown that treatment with statins resulted in a protective effect on the progression of cardiomyopathy during the chronic stages of infection in a dog model [10]. Many factors including the animal models used, parasite strain, stage of infection and the amount of drug used could have accounted for the differences in experimental outcomes between this study and the previous study [10]. Atorvastatin treatment in uninfected mice also demonstrated a significant increase in the scavenger receptors, metabolic mediators and inflammatory markers (mRNA analysis) in HFDA fed mice compared to RDA fed mice (Supplemental Fig. 1&2). To this end, while the current acute infection study in mice demonstrates that atorvastatin treatment has several deleterious effects on the acute infection, there were some positive effects of atorvastatin in acute infection demonstrated by MRI, illustrating the complexity of this pathogenic process.

Similarly to WAT, in the heart tissues of atorvastatin treated mice, LDL receptor protein levels were significantly higher during the active acute phase of infection (d20 pi) compared to untreated mice. The cardiac LDL receptor levels in atorvastatin-treated HFD fed infected mice were significantly higher (15 fold) compared to atorvastatin-treated RD fed mice. Because atorvastatin is known to increase intracellular LDL receptor levels [12], this increase may at least partially underlie the tissue increases in parasite loads in atorvastatin-treated mice. Overall, this suggests that atorvastatin treatment induced LDL receptor and other scavenger receptors probably contributed to the increased cardiac parasite loads in treated infected mice. Interestingly, Cxcl16, an oxidized LDL receptor binding scavenger receptor expressed mainly on macrophages, was expressed more highly in the hearts of atorvastatin-treated mice at the end of acute phase (d30 pi), suggesting that oxidized LDL could play a major role in the pathogenesis of acute myocarditis observed in Chagas disease. In support of this idea, other groups have noted that oxidative stress may be an important factor in the development of Chagasic cardiomyopathy (18, 19).

Treatment with atorvastatin also increased adipose tissue lipolysis resulting in cardiac inflammation, parasite load and lipid accumulation. Increased LDL receptors and other scavenger receptors in atorvastatin treated mice likely played a major role in the pathogenesis of acute infection in this mouse model. Together, these results indicate that cholesterol-lowering drugs may adversely affect the pathology and outcomes of acute Chagas disease.

Histological data at d30 pi demonstrated an increase in inflammation in the hearts of atorvastatin treated mice compared with their respective atorvastatin untreated mice (Figure 2). Levels of inflammatory cells were lower in HFDA fed infected mice compared with RDA fed infected mice, consistent with the previously observed protective effect of HFD on inflammation in the heart [2]. qPCR data also confirmed the decreased levels of inflammatory markers in the hearts of HFDA fed mice compared to RDA fed mice at d30 pi. However, at the same time point inflammatory markers were significantly higher in the WAT of HFDA compared to RDA fed mice. This difference suggests that atorvastatin and HFD are likely to have different mechanisms in WAT and heart in the regulation of inflammatory markers during acute infection. These mechanisms likely have important physiological consequences because WAT can be a source of systemic inflammatory markers and persistent inflammation in WAT is associated with obesity (20, 21).

Lipolysis is a key marker of acute Chagas disease [2, 4]. Previously we reported that different lipases play a major role in the loss of fat cells during acute infection in the mice fed on a routine mouse chow diet [2, 4]. In particular, protein levels of HSL and ATGL are significantly increased and decreased, respectively, in the WAT of mice fed on chow diet at d15pi [4]. Here we found that HSL is significantly decreased and ATGL is significantly increased in both RD and HFD fed mice during early acute phase of infection (d10pi) in untreated mice which suggests that diet could regulate the levels of lipases during infection. Atorvastatin treatment significantly decreases HSL in uninfected mice. In contrast, atorvastatin increased HSL in infected mice compared to untreated mice (Fig. 4). ATGL levels were significantly increased compared to uninfected mice during infection irrespective of the diet and atorvastatin treatment (Fig. 4). Lipitor significantly increased ATGL in uninfected mice in both RD and HFD fed mice. However, atorvastatin significantly increased ATGL only in RD infected mice and not in HFD infected mice. This result suggests that atorvastatin has a differential regulatory effect on lipase levels in RD and HFD fed mice. Interestingly, it was also previously shown that levels of insulin, a key regulator of lipases, are altered during acute infection [22, 23]. Thus, further investigation is needed to understand the mechanism(s) underlying the interaction of atorvastatin with insulin signaling during infection.

Previously a beneficial effect of HFD on adipogenesis of WAT was demonstrated in acute murine Chagas model [2]. Atorvastatin treatment further enhanced the levels of adipogenesis markers such as adiponectin, adipogenin, leptin and Ppar-γ in WAT (Figure 4). Even though parasite loads were higher in WAT and hearts from HFDA fed infected mice compared to RDA fed infected mice, HFDA fed mice had an improved survival rate over RDA fed mice during acute infection. This suggests that HFD by itself plays a major role in reducing mortality either by improving the physiology of adipose tissue or by reducing cardiac inflammation. In support of this idea, cholesterol efflux markers such as Apoa, Apob, Abca1 and Abcg1 were more highly expressed in the WAT of HFDA fed infected mice compared to RDA fed infected mice (Table 2). Also, cholesterol and fatty acid metabolism was significantly higher in the WAT of HFDA fed infected mice compared to RDA fed infected mice, as measured by qPCR (Tables 2 &3). Thus, our results indicate that atorvastatin treatment plays a major role in the regulation of adipogenesis in WAT during *T. cruzi* infection in HFD fed mice.

The dual epidemic of diabetes and obesity in the endemic regions of Chagas disease is constantly increasing and many of these patients have hyperlipidemia and are on atorvastatin treatment. The interaction of endemic tropical diseases with the epidemic of diabetes and obesity is a neglected area of research, but this interaction may have a significant effect on the pathogenesis of these endemic tropical diseases. Our data provide experimental evidence that atorvastatin treatment may lead to an adverse outcome in acute infection for humans on this compound and may lead to an increased risk of cardiomyopathy in people on atorvastatin who have an acute *T. cruzi* infection. This hypothesis will need to be evaluated by clinical epidemiological studies in endemic regions.

Supplementary Material

Refer to Web version on PubMed Central for supplementary material.

ACKNOWLEDGEMENT

This study was supported by grants from the National Heart, Lung, and Blood Institute (National Institutes of Health HL-112099 and HL-122866) to Jyothi Nagajyothi.

REFERENCES

1. Montgomery SP, Starr MC, Cantey PT, Edwards MS, Meymandi SK. Neglected parasitic infections in the United States: Chagas disease. Am J Trop Med Hyg. 2014; 90:814–8. [PubMed: 24808250]
2. Nagajyothi F, Weiss LM, Zhao D, Koba W, Jelicks LA, Cui MH, et al. High fat diet modulates *Trypanosoma cruzi* infection associated myocarditis. PLoS Negl Trop Dis. 2014; 8:e3118. [PubMed: 25275627]
3. Combs TP, Nagajyothi F, Mukherjee S, de Almeida CJ, Jelicks LA, Schubert W, et al. The adipocyte as an important target cell for *Trypanosoma cruzi* infection. J Biol Chem. 2005; 280:24085–94. [PubMed: 15843370]
4. Nagajyothi F, Desruisseaux MS, Machado FS, Upadhya R, Zhao D, Schwartz GJ, et al. Response of adipose tissue to early infection with *Trypanosoma cruzi* (Brazil Strain). J Infect Dis. 2012; 205:830–40. [PubMed: 22293433]
5. Brima W, Eden DJ, Mehdi SF, Bravo M, Wiese MM, Stein J, et al. The brighter (and evolutionarily older) face of the metabolic syndrome: evidence from *Trypanosoma cruzi* infection in CD-1 mice. Diabetes Metab Res Rev. 2015; 31:346–59. [PubMed: 25613819]
6. Nagajyothi F, Zhao D, Weiss LM, Tanowitz HB. Curcumin treatment provides protection against *Trypanosoma cruzi* infection. Parasitol Res. 2012; 10:2491–99.
7. Johndrow C, Nelson R, Tanowitz H, Weiss LM, Nagajyothi F. *Trypanosoma cruzi* infection results in an increase in intracellular cholesterol. Microbes Infect. 2014; 16:337–44. [PubMed: 24486184]
8. Nagajyothi F, Weiss LM, Silver DL, Desruisseaux MS, Scherer PE, Herz J, et al. *Trypanosoma cruzi* utilizes the host low density lipoprotein receptor in invasion. PLoS Negl Trop Dis. 2011; 5:e953. [PubMed: 21408103]
9. International Diabetes Federation. [6 May 2013] IDF Diabetes Atlas. sixth edition2013. http://www.idf.org/sites/default/files/EN_6E_Atlas_Full_0.pdf
10. Melo L, Caldas IS, Azevedo MA, Gonçalves KR, do Nascimento AF, Figueiredo VP, et al. Low doses of simvastatin therapy ameliorate cardiac inflammatory remodeling in *Trypanosoma cruzi*-infected dogs. Am J Trop Med Hyg. 2011; 84:325–31. [PubMed: 21292909]
11. Durand JL, Tang B, Gutstein DE, Petkova S, Teixeira MM, Tanowitz HB, et al. Dyskinesis in Chagasic myocardium: centerline analysis of wall motion using cardiac-gated magnetic resonance images of mice. Magn Reson Imaging. 2006; 24:1051–57. [PubMed: 16997075]

12. Pocathikorn A, Taylor RR, Mamotte CD. Atorvastatin increases expression of low-density lipoprotein receptor mRNA in human circulating mononuclear cells. Clin Exp Pharmacol Physiol. 2010; 37:471–76. [PubMed: 19930424]
13. Pereira IR, Vilar-Pereira G, Silva AA, Moreira OC, Britto C, Sarmento ED, et al. Tumor necrosis factor is a therapeutic target for immunological unbalance and cardiac abnormalities in chronic experimental Chagas' heart disease. Mediators Inflamm. 2014; 2014:798078. [PubMed: 25140115]
14. Lannes-Vieira J, Pereira IR, Vinagre NF, Arnez LE. TNF-α and TNFR in Chagas disease: from protective immunity to pathogenesis of chronic cardiomyopathy. Adv Exp Med Biol. 2011; 691:221–30. [PubMed: 21153326]
15. Ahn KS, Sethi G, Aggarwal BB. Simvastatin potentiates TNF-α-induced apoptosis through the down-regulation of NF-κB-dependent antiapoptotic gene products: role of IκBα kinase and TGF-β-activated kinase-1. J Immunol. 2011; 178:2507–16.
16. Prioli RP, Rosenberg I, Pereira ME. High- and low-density lipoproteins enhance infection of *Trypanosoma cruzi* in vitro. Mol Biochem Parasitol. 1990; 15:191–98.
17. Miao Q, Ndao M. *Trypanosoma cruzi* Infection and host lipid metabolism. Mediators Inflamm. 2014; 2014:902038. [PubMed: 25276058]
18. Wen J-J, Dhiman M, Whorton EB, Garg NJ. Tissue-specific oxidative imbalance and mitochondrial dysfunction during *Trypanosoma cruzi* infection in mice. Microbes Infect. 2008; 10:1201–9. [PubMed: 18675934]
19. Dhiman M, Estrada-Franco JG, Pando JM, Ramirez-Aguilar FJ, Spratt H, Vazquez-Corzo S, et al. Increased Myeloperoxidase Activity and Protein Nitration Are Indicators of Inflammation in Patients with Chagas'Disease. Clin Vaccine Immunol : Clin Vaccine Immunol. 2009; 16:660–6. [PubMed: 19297613]
20. Makki K, Froguel P, Wolowczuk I. Adipose tissue in obesity-related inflammation and insulin resistance: cells, cytokines, and chemokines. ISRN inflamm. 2013; 22:139239.
21. Sun K, Kusminski CM, Scherer PE. Adipose tissue remodeling and obesity. J Clin Invest. 2011; 121:2094–101. [PubMed: 21633177]
22. Nagajyothi F, Kuliawat R, Kusminski CM, Machado FS, Desruisseaux MS, Zhao D, et al. Alterations in glucose homeostasis in a murine model of Chagas disease. Am J Pathol. 2013; 182:886–94. [PubMed: 23321322]
23. Choi SM, Tucker DF, Gross DN, Easton RM, DiPilato LM, Dean AS, et al. Insulin regulates adipocyte lipolysis via an Akt-independent signaling pathway. Mol Cell Biol. 2010; 30:5009–20. [PubMed: 20733001]

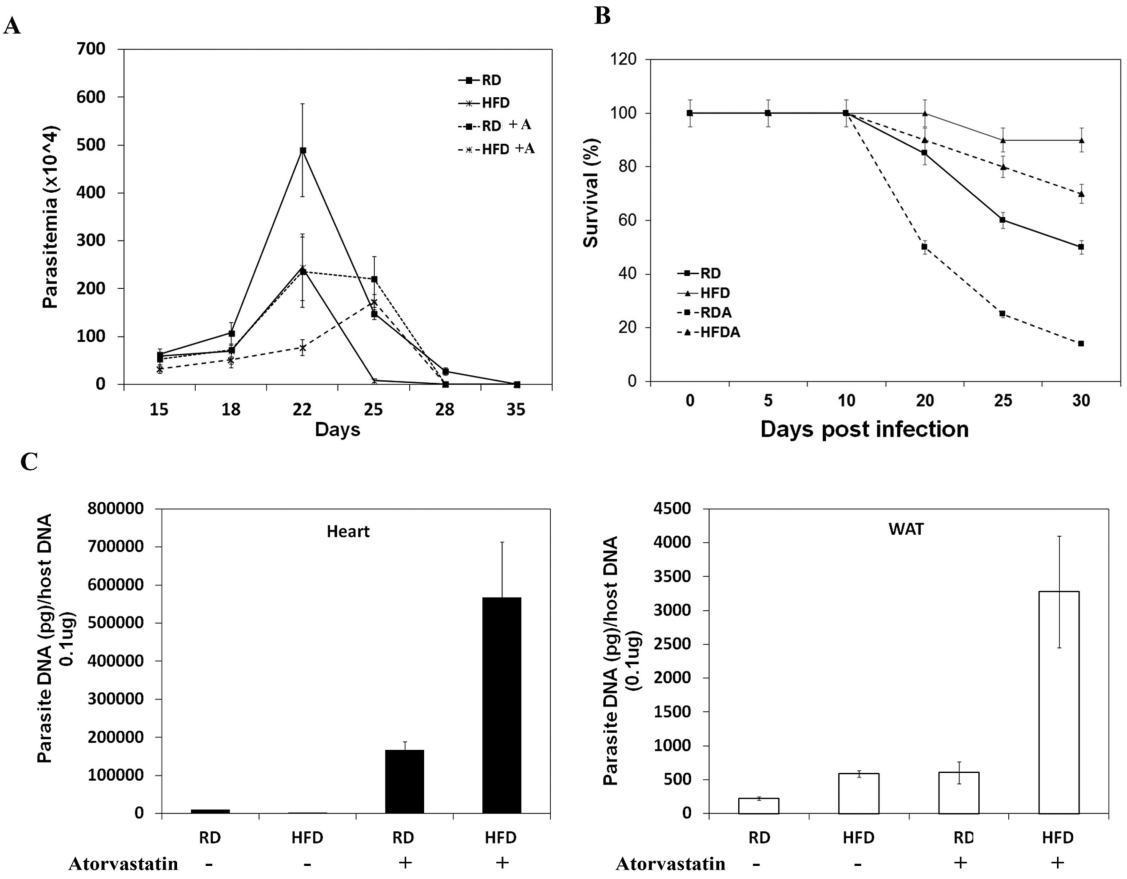

Figure 1. Atorvastatin treatment enhances the mortality rate and tissue parasite loads in mice during acute *T. cruzi* infection (n=30)

A. Mice fed on atorvastatin-supplemented diets (RDA & HFDA) showed less than a two-fold decrease in parasitemia compared to mice fed on a diet without atorvastatin (RD & HFD) at d22pi.

B. Mice fed on atorvastatin-supplemented diets (RDA & HFDA) showed a significantly reduced survival rate (14 and 68% respectively) compared to uninfected mice (100%). Mice fed on RD and HFD without atorvastatin (RD &HFD) showed 45 and 90% survival rate during acute infection.

C. qPCR analysis demonstrated a significant increase (3.4-fold) of parasites in the hearts of HFDA fed infected mice compared to RDA fed infected mice. Infected mice from both the atorvastatin treated groups (HFDA & RDA) showed significantly higher parasite loads compared to untreated mice (251 and 15.7-fold respectively). WAT from mice fed on atorvastatin-supplemented diets demonstrated significantly higher parasite loads compared to mice fed on a diet without atorvastatin (parasite load in HFDA is increased 5.5-fold compared to HFD mice and parasite load in RDA is increased 2.7-fold compared to RD mice).

$p \leq 0.005$, represented by black stars. Bars represent mean values of the data with Standard Error of the mean (SEM) as vertical lines. RD – regular diet; HFD-high fat diet; RDA - atorvastatin-supplemented regular diet; HFDA - atorvastatin-supplemented high fat diet.

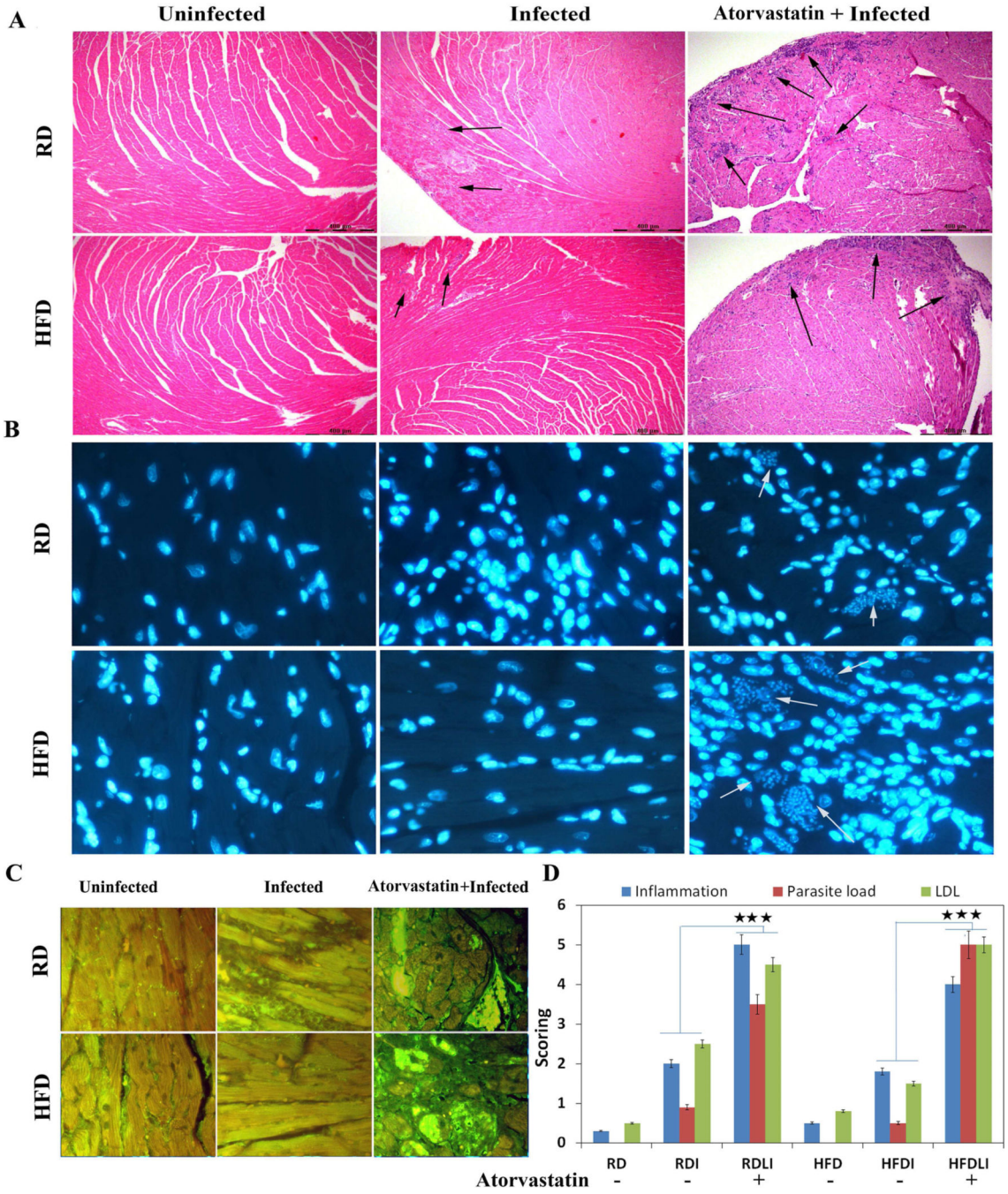

Figure 2. Histological and immunofluorescence analysis of the myocardium of mice during acute infection (d30 pi)

A. Atorvastatin treatment significantly increased myocardial inflammation and damage (black arrow) in infected mice compared to untreated infected mice as demonstrated by H&E staining. Inflammation was significantly greater in RDA fed infected mice compared to HFDA fed infected mice.

B. Atorvastatin treated infected mice displayed the presence of amastigote nests (white arrow) in myocardium irrespective of the diets fed as demonstrated by DAPI staining. HFDA fed infected mice showed a greater number and larger sized amastigote nests in the

myocardium compared to RDA fed infected mice. However, in untreated infected mice (fed on RD or HFD), amastigote nests were not easily detectable by DAPI staining (however, individual parasites were observed).

C. Increased LDL accumulation in the myocardium of atorvastatin treated infected mice was observed compared to untreated mice as demonstrated by Immunofluorescence analysis (IFA) using LDL antibody. Myocardium of HFDA fed mice showed higher levels of LDL compared to RDA fed mice at d30 pi.

Histological and analytical grading of inflammation (H&E staining), presence of amastigote nests (DAPI staining), and LDL accumulation (anti-LDL IFA) were carried out as previously described [2]. Five images from each section were analyzed. The cardiac LDL levels of the IFA images were quantified using Image J program (NIH) and represented as a bar graph (fold change is converted to scores). Each class was graded on a six point scale ranging from 0 to 5+, and presented as a bar graph for H&E and DAPI staining. Bars represent mean values of the data with standard error of the mean (SEM) as vertical lines. Inflammation (blue), parasite load (red) and LDL levels (green) were significantly higher in atorvastatin treated infected mice compared to untreated infected mice (represented by stars, ≤ 0.005). Between the two groups of atorvastatin treated infected mice, inflammation was significantly higher in RDA fed mice and parasite load and LDL levels were greater in HFDA fed mice.

For all studies 5 mice were examined in each group and a minimum of five images/sections were analyzed for each mouse (i.e. 25 sections per group).

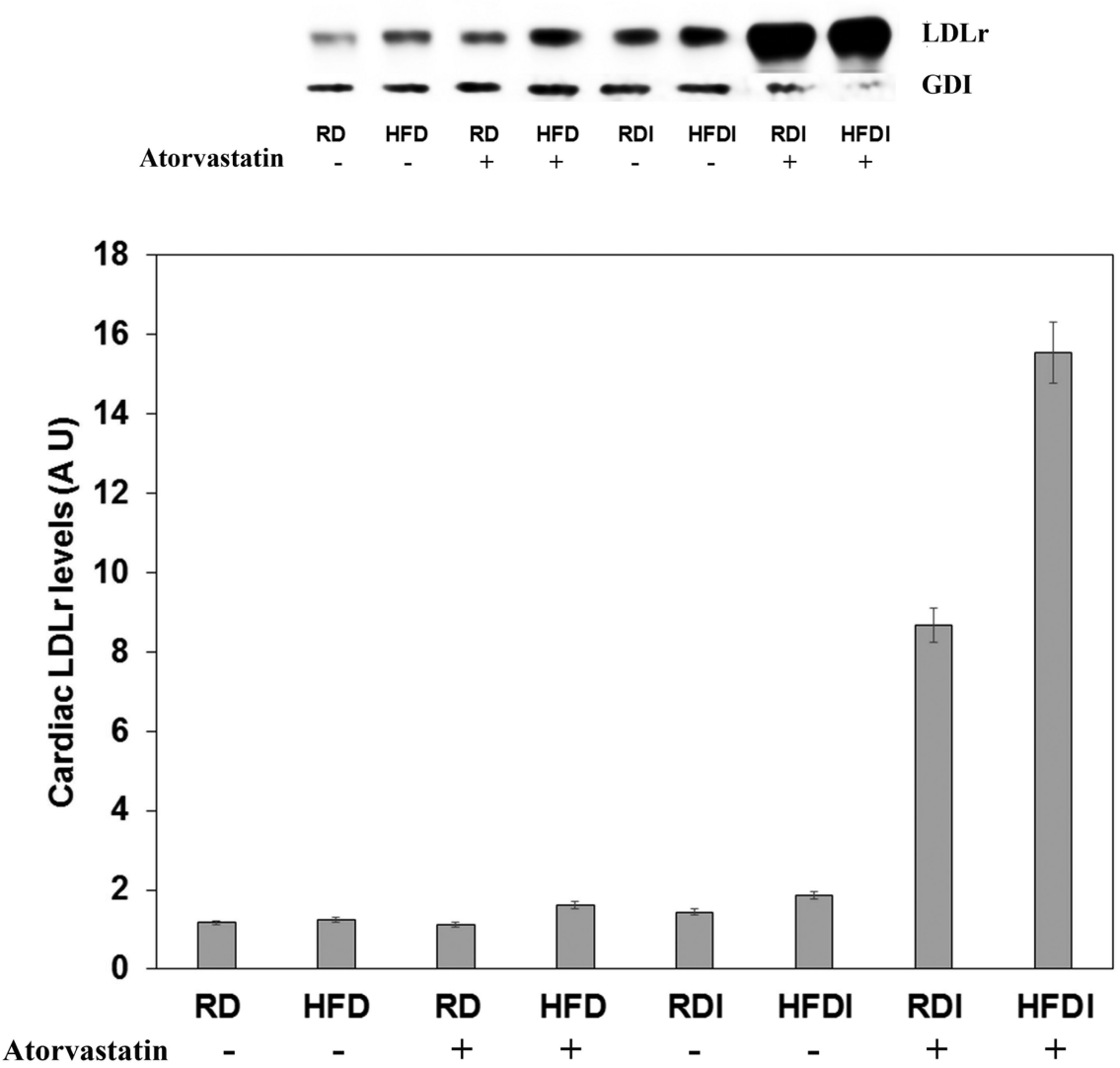

Figure 3. Atorvastatin alters LDL receptor levels during acute *T. cruzi* infection in heart

Immunoblot analysis using anti-rabbit LDL receptor antibody demonstrated that infection and atorvastatin treatment independently and synergistically increased the expression of LDL receptors in the mouse hearts. Thus, HFDA fed infected mice showed the highest cardiac levels of LDL receptor compared to all the experimental groups. Fold change in the protein levels were normalized to GDI expression and represented as bar graph (n=5, $p \leq 0.005$). Bars represent mean values of the data with SEM as vertical lines. Significant change is represented by stars.

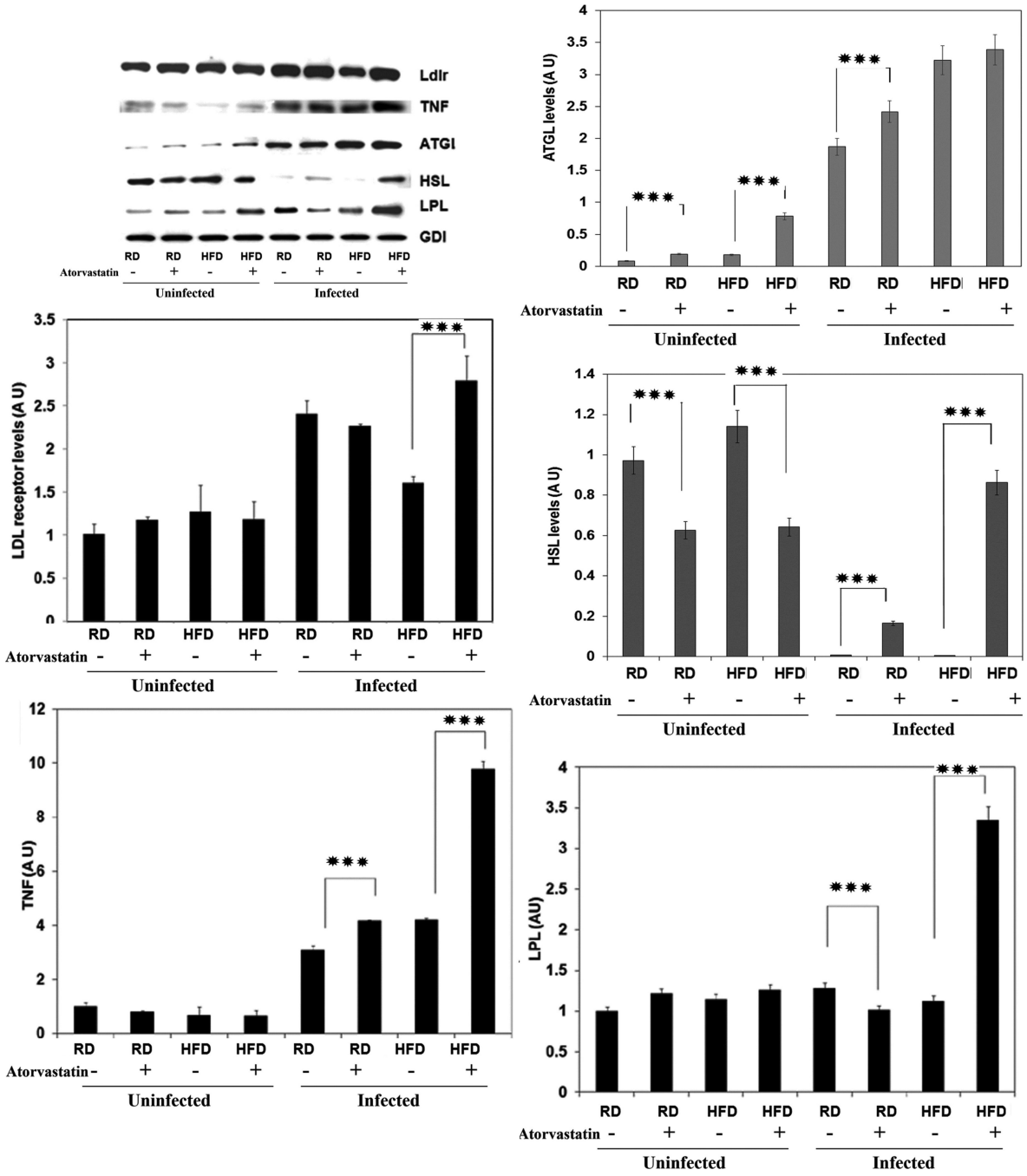

Figure 4. Atorvastatin treatment affects *T. cruzi* infection-induced systemic alterations in the protein levels of LDL receptor, TNFα and lipases in white adipose tissue (WAT)

WAT from all the uninfected and infected mice groups (RD, HFD, RDA and HFDA fed mice) at d10 pi were analyzed for the protein levels of LDL receptor, TNFα, and lipases (ATGL, HSL and LPL). Fold change in the protein levels were normalized to GDI expression and represented as bar graph (n=5, p≤0.005). The levels of LDL receptor were significantly increased in WAT of all the infected groups compared to uninfected groups. Atorvastatin treatment synergistically increased LDL receptor levels in HFDA fed infected mice compared to untreated HFD fed mice. Atorvastatin treatment also significantly

increased TNFα levels in the infected mice fed on either RD or HFD. Atorvastatin treatment significantly increased ATGL levels and decreased HSL levels in WAT of infected mice compared to uninfected mice regardless of the type of diet. However, atorvastatin treatment decreased ATGL in RD fed mice but increased HSL in HFD mice. Atorvastatin treatment also inversely altered LPL levels in RD and HFD fed infected mice, decreasing them in RD mice and increasing them in HFD mice. Bars represent mean values of the data with SEM as vertical lines. Significant change is represented by black stars compared with uninfected RD mice. Significant difference between infected RD and infected HFD is represented by white stars ($p \leq 0.005$).

Table 1

MRI analysis demonstrated the effect of Atorvastatin treatment on the altered ventricle diameter, wall thickness and fractional shortening in the hearts of *T. cruzi* infected mice fed on regular or high fat diet (n=5 ; data presented as Mean ± SEM).

Mice	LVID (Diastole)	LVID (Systole)	RVID (Diastole)	RVID (Systole)	Wall average	%FS
RD Control	4.5±0.1	2.2±0.1	2.1±0.09	1.1±0.0	2.4±0.04	49.8±0.6
HFD Control	4.2±0.2	1.7±0.1	1.9±0.1	0.9±0.5	2.0±0.1	61.3±3.01
RD Infected	3.2±0.1	0.8±0.12	2.8±0.1	2.4±0.1	3.5±0.1	74.9±3.2
RDA Infected	4.45±0.1	2.5±0.14	1.6±0.1	0.96±0.05	1.0±0.1	42.9±2.7
HFD Infected	3.6±0.01	1.1±0.18	2.9±0.1	2.1±0.03	2.1±0.03	64.3±2.3
HFDA infected	3.8±0.1	1.5±0.11	2.2±0.1	1.8±0.2	1.1±0.01	60.5±1.7

Table. 2

Fold change (Mean ± SEM) in the mRNA levels of the genes for Lipoprotein metabolism, cholesterol efflux, adipogenesis, fat metabolism and inflammation in WAT and heart of *T. cruzi* infected mice fed on a atorvastatin treated regular or high fat diet (RDA or HFDA) compared to their respective atorvastatin untreated regular or high fat diet (RD or HFD) .

Gene list	White adipose tissue (WAT)		Heart	
	RDA Infected	HFDA Infected	RDA Infected	HFDA Infected
Cxcl16	−108.8 ± 6.8	993. ± 83	232 ± 62	216 ± 38
Stabl	2.6 ± 0.3	2600. ± 262	−8.1 ± 2.3	1.5 ± 0.2
Vldlr	5.2 ± 1.1	0.15 ± 0.03	−5.5 ± 1.1	3.3 ± 0.9
Ldlr	−1.2 ± 0.03	2596 ± 198	−1.7 ± 0.3	−1.8 ± 0.4
Scarf1	−1.1 ± 0.1	181960 ± 7800	1.6 ± 0.2	1.2 ± 0.2
Apo a1	−1.1 ± 0.1	9568 ± 980	−7.4 ± 1.3	11.44 ± 2.1
Apo b	1.5 ± 0.2	179598 ± 12900	−3.5 ± 1.0	109 ± 10
Apo e	1.1 ± 0.1	0.52 ± 0.004	1.1 ± 0.1	−1.0 ± 0.04
Abc a1	−2344 ± 320	3619 ± 860	1.6 ± 0.2	−223513 ± 9890
Abc g1	−1.7 ± 0.3	183 ± 32	1.6 ± 0.1	−1.3 ± 0.03
Lep	−2.7 ± 0.1	93.0 ± 8.7	1.7 ± 0.4	1.6 ± 0.4
Ppara	1.0± 0.1	1814 ± 121.0	−3.4 ± 0.5	−1.1 ± 0.02
Pparg	−1.8 ± 0.2	75.3 ± 12.7	−2.0 ± 0.1	−1.0 ± 0.1
Adig	−2.2 ± 0.2	137± 21.1	−1.5 ± 0.3	−1.2 ± 0.3
Adiponectin	−2.4 ± 0.3	3.3 ± 0.9	2.6 ± 0.3	−3.2 ± 0.7
Npc1	−1.08 ± 0.02	22.3 ± 3.4	−1.4 ± 0.2	−1.4 ± 0.01
Cyp39a1	1.7 ± 0.3	1050 ± 62	−2.7 ± 0.3	−1.3 ± 1.0
Cyp7a1	1.2 ± 0.6	2529 ± 198	4.7 ± 0.8	175 ± 16
Hmgcr	−1.5 ± 0.1	2.8834 ± 0.4	1.1 ± 006	−1.6 ± 0.5
Hmgcs1	−2.3 ± 0.9	24 ± 6	−1.4 ± 0.1	−1.3 ± 0.03
Acaa1a	−1.3 ± 0.1	2.4 ± 0.4	−1.7 ± 0.3	−1.6 ± 0.1
Acad9	−1.1 ± 0.03	14.7 ± 3.2	−1.2 ± 0.01	−1.7 ± 0.5
Acad10	1.8 ± 0.04	21.4± 2.8	−1.0 ± 0.1	1.2 ± 0.3
Acox1	−1.8 ± 0.3	126. ± 28	−2.3 ± 0.8	−1.4 ± 0.3
Fabp1	1.4 ± 0.3	19715 ± 623	−2.7 ± 0.7	4.4 ± 0.9
Ccl2	−2.9 ± 0.9	209 ± 33	1.7 ± 0.5	−1.3 ± 0.03
Ccl5	3.4 ± 0.5	931 ± 121	2.6 ± 0.1	−2.0 ± 0.4
Ccr1	1.1 ± 0.1	6.6 ± 1.	2.9 ± 0.9	−1.0 ± 0.05
Ccr2	2.4 ± 0.4	165 ± 13	1.2 ± 0.003	−3.5 ± 0.3
Ifng	9.5 ± 1.2	481 ± 66	1.8 ± 0.02	−1.5 ± 0.2
Il1a	1.1 ± 0.4	353 ± 33	3.4 ± 1.0	1.5 ± 0.3
Itgb2	−2.3 ± 0.02	0.7 ± 0.02	2.3 ± 0.4	−1.8 ± 0.3
Tgfb1	−1.6 ± 0.1	6777 ± 976	1.5 ± 0.02	−1.4 ± 0.07
Tnf	1.7 ± 0.1	3117 ± 328	3.0 ± 0.1	1.0 ± 0.009

The gene expression levels of RDA fed infected mice are compared to RD fed infected mice and the gene expression levels of HFDA fed infected mice are compared to HFD fed infected mice.